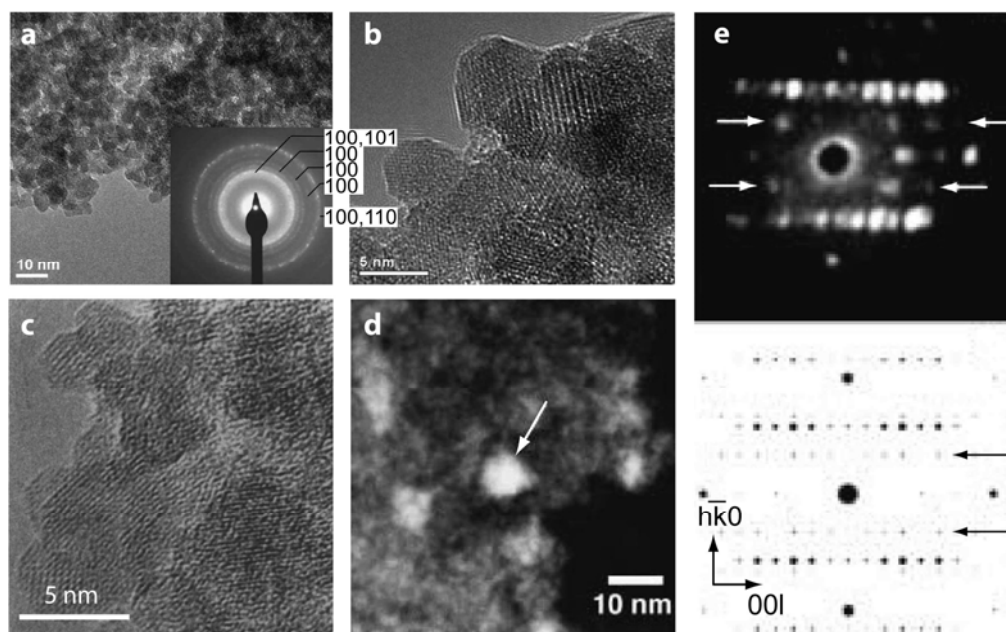


## Supplement for the article :

### Critical evaluation of the revised akdalaite-model for ferrihydrite

A. MANCEAU

#### Some published TEM results supporting the standard model



**Figure S1.** (a-c) Examples of HRTEM images of six-line ferrihydrite grains showing commonly observed rounded to hexagonal shapes. (d) Annular dark-field STEM images of coherently diffracting domains. The arrow points to a 10 nm single domain. (e) Nanodiffraction pattern for the [110] orientation of the f-phase with simulated pattern from the standard model. Arrows point out extra spots from the superlattice structure described by Drits et al. (1993). After Pan et al. (2006) and Janney et al. (2000, 2001).

#### Fe coordination from PDF and the violation of Pauling's 2<sup>nd</sup> rule

The coordination of Fe can be assessed from PDF by calculating the average Fe-O bond length because, (1), the lengths were regressed from the first PDF peak which contains all possible Fe-O correlations, (2), the presence of tetrahedral iron (<sup>IV</sup>Fe) should shift this value to a shorter distance. The averages for the two successive akdalaite models are slightly different  $\langle d(\text{Fe-O})_{\text{ferrifh}} \rangle = 2.017 \text{ \AA}$  and  $\langle d(\text{Fe-O})_{\text{fhyd6}} \rangle = 2.00 \text{ \AA}$ , which is consistent with the fact that the PDFs were derived from different materials. The average Fe-O distance for the more recent ferrifh model matches exactly the average value of  $2.015 \text{ \AA}$  for <sup>VI</sup>Fe<sup>3+</sup> obtained from a survey of 204 Fe-O binding environments in the Inorganic Crystal Structure Database (Brown and Altermatt 1985). The average value for <sup>IV</sup>Fe<sup>3+</sup> is shorter at  $1.865 \text{ \AA}$ . If ferrihydrite contained 20% <sup>IV</sup>Fe, as in the akdalaite model, the average PDF bond length would be approximately  $1.985 \text{ \AA}$ , not  $2.017 \text{ \AA}$  and  $2.00 \text{ \AA}$ , a difference that can be resolved by HEXS (Wells et al. 2009), especially with the precision on bond lengths of  $10^{-3} \text{ \AA}$  reported by Michel et al. (2010). In addition, the higher metrical value of ferrifh suggests that the maghemite phase contained in hydromaghemite had little <sup>IV</sup>Fe, in agreement with previous studies (Liu et al. 2008; de Boer and Dekkers 2001).

The average Fe-O distance of 2.017 Å obtained by regression analysis of the PDF data for hydromaghemite (i.e., ferrifh sample) is likely correct because this value was constrained by the position of the maximum of the Fe-O correlations in the PDF. Because Michel et al. (2010) fit their data with a model structure based on that of akdalaite ( $\text{Al}_{10}\text{O}_{14}(\text{OH})_2$ ), which contains 20%  $^{\text{IV}}\text{Al}$ , the optimized distribution of Fe-O distances was forced to include this coordination. In Fig. 4c of Michel et al. (2010) the calculated partial PDF for the  $^{\text{IV}}\text{Fe}3$  atoms has a weak peak at  $R \sim 1.8$  Å that was attributed consistently to the  $^{\text{IV}}\text{Fe}3\text{-O}4$  correlation at 1.816 Å in the crystallographic model. The next peak observed at  $\sim 2.0$  Å was attributed to the three O2 needed to complete the tetrahedral coordination of  $^{\text{IV}}\text{Fe}3$ . However, this peak was listed by Michel et al. (2010) as occurring at 1.932 Å instead of  $\sim 2.0$  Å (the comparable value is 2.02 Å in fhyd6). Therefore, the weak contribution of one Fe-O distance at  $\sim 1.8$  Å, out of a total of 28 (Fig. 4e) in the simulation of the ferrifh PDF, is the only evidence for  $^{\text{IV}}\text{Fe}$ . This contribution is clearly too small to be statistically significant; it was imposed by the akdalaite model to satisfy the preconceived  $^{\text{IV}}\text{Fe}$  coordination. This is an illustration of a model-dependent optimization problem, which the PDF technique is prone to (Farrow et al. 2007; Manceau 2010).

The violation of Pauling's 2<sup>nd</sup> rule by the previous fhyd6 model was reportedly fixed in the new ferrifh model. Using the  $^{\text{IV}}\text{Fe}3\text{-O}$  distances of 1.82 and  $\sim 2.0$  Å in Figure 4c of Michel et al. (2010) and the same bond-valence method as the authors (Brown and Altermatt 1985),  $^{\text{IV}}\text{Fe}3$  receives approximately  $0.85 + 0.52 \times 3 = 2.41$  v.u. from the O4 and three O2 oxygens, not 2.74 as misrepresented in their Table S4. The valence sum problem does not seem to have been completely solved by the ferrifh model, which appears to violate both Pauling's 2<sup>nd</sup> and distortion rules.

Lastly, Xu et al. (2011) observed by PDF that the first shell Fe-O distance decreases from 1.99 Å to 1.96 Å when ferrihydrite is transformed to hematite upon heating. This reduction of the average Fe-O distance with temperature is a strong argument against the presence of tetrahedral Fe in ferrihydrite. If Fh contained 20%  $^{\text{IV}}\text{Fe}$  as in the akdalaite-like model, then the average Fe-O bond length could only increase with temperature because hematite has only octahedral Fe. A tetrahedron is smaller than an octahedron, therefore a reduction of distance is inconsistent with a coordination change from tetrahedral to octahedral.

### EXAFS data of akaganeite at room and liquid nitrogen temperatures

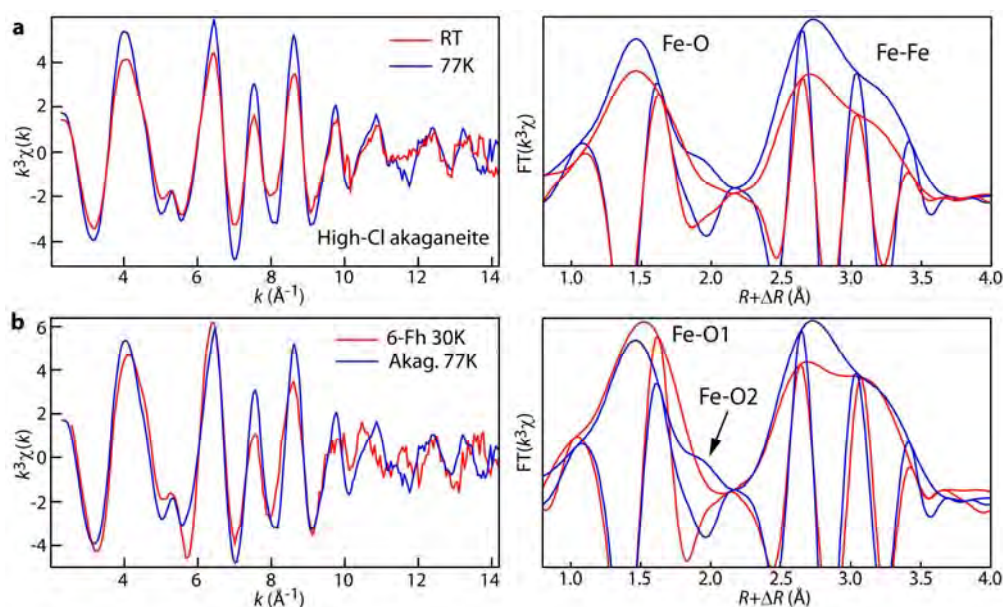


**Figure S2.** EXAFS (left) and Fourier transforms (right) for high-Cl akaganeite at room and liquid nitrogen temperatures (a), and for high-Cl akaganeite at 77K and six-line ferrihydrite at 30K (b). Akaganeite was prepared by neutralizing to neutral pH a 0.1 M FeCl<sub>3</sub> solution.

Lowering the temperature increases the sensitivity of EXAFS to the long Fe-O distances at 2.10-2.20 Å in both akaganeite and ferrihydrite. Ferrihydrite has a mean Fe-O1 distance of  $R = 1.98$  Å (after correction of the  $\Delta R$  phase shift) and akaganeite  $R = 1.95$  Å (Table 1). A distance of 1.98 Å for 6Fh is the value usually reported in the literature. The difference to the nominal 2.01 Å value for <sup>VI</sup>Fe does not mean that ferrihydrite contains <sup>IV</sup>Fe, but that EXAFS analysis from room temperature data excludes the full distribution of interatomic distances.

### Multiple versus single shell EXAFS analysis

The contributions to EXAFS of the Fe-O and Fe-Fe pairs were fit simultaneously in  $k$  space with WinXAS v. 3.2 (Ressler, 1998). Theoretical backscattering phases and amplitudes were calculated with FEFF v. 7 (Ankudinov and Rehr 1997) using goethite as structural model (Hazemann et al. 1991). The  $R + \Delta R$  window of the Fourier backtransforms varied from 0.9-3.5 Å to 0.9-3.7 Å. The procedure used to calculate the confidence limits for  $CN_j$ ,  $R_j$  and  $\sigma_j$  reported in Table S1 is described in Ressler et al. (2010).

Caution is advocated to not analyze separately the anionic (O) and cationic (Fe) shells in  $k$  space, in particular the Fe-O pair because its contribution partly overlaps with the most intense Fe-Fe wave function. The importance of truncation errors introduced by a shell-by-shell analysis of ferrihydrite is evaluated below with the theoretical spectrum of goethite (Fig. 3 of Manceau 2009), and with the experimental data of feroxyhite and 6Fh. Fitting a model spectrum (i.e., goethite) provides unambiguous information about the reliability of the EXAFS data-analysis procedure.

Truncation effects on data itself caused by the finite data range and overlapping shells is illustrated in Figure S3a with the single scattering  $\chi_{\text{Fe-O}}$  function of goethite, (1), calculated directly with FEFF, and (2), Fourier-filtered from the total *ab initio* EXAFS spectrum. The two functions are clearly not the same, showing distinct differences in shape and wave frequency at several  $k$  values. In agreement with theory, the least-squares fit spectrum is superimposed on the unfiltered  $\chi_{\text{Fe-O}}$  function, and the regressed parameters are identical to crystallographic values used to calculate  $\chi_{\text{Fe-O}}$  (Fig. S3b). When the analysis is performed on the Fourier filtered function, the best-fit parameters are in close proximity to crystallographic values only if the two Debye-Waller terms ( $\sigma_{\text{O1}}$  and  $\sigma_{\text{O2}}$ ) or coordination numbers ( $CN_{\text{O1}}$  and  $CN_{\text{O2}}$ ) are constrained to the same value during minimization (Fig. S3c). Otherwise, if  $\sigma_{\text{O1}} \neq \sigma_{\text{O2}}$  and  $CN_{\text{O1}} \neq CN_{\text{O2}}$ , then  $R_{\text{O1}}$  and  $R_{\text{O2}}$  decrease by 0.03-0.04 Å and the fit is improved due to the higher number of degrees of freedom in the regression (Fig. S3d).

The influence of the Fourier transform truncation on the fit variances of feroxyhite and 6Fh are shown in Figure S4. Results show that truncation effects are even more important in disordered materials. In both cases, an unrealistic distance of 1.87 Å is obtained when neither  $\sigma$  nor  $CN$  are constrained, and statistical tests show considerable covariance of some fit parameters.

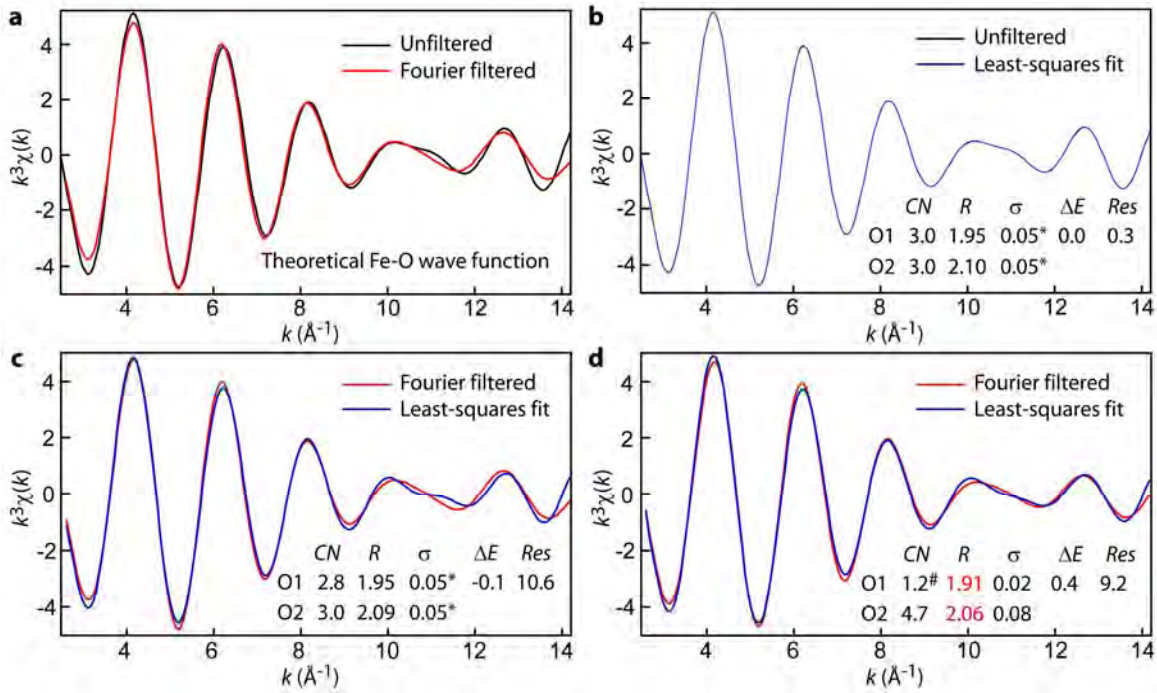


**Figure S3.** (a) Theoretical  $\chi_{\text{Fe-O}}$  wave function for goethite calculated with FEFF v. 7 (unfiltered) and Fourier-filtered from the total *ab initio* EXAFS spectrum. The theoretical electronic wave was calculated using the following crystallographic values for the first atomic shell:  $R_{O1} = 1.95 \text{ \AA}$ ,  $R_{O2} = 2.10 \text{ \AA}$ ,  $\sigma = 0.005 \text{ \AA}$ . Additional details can be found in Manceau (2009). (b-d) Least-squares fits and best-fit values of the unfiltered and Fourier-filtered  $\chi_{\text{Fe-O}}$  functions. When  $\sigma_{O1}$  and  $\sigma_{O2}$  are optimized independently (d), several parameters are strongly correlated and the minimization algorithm converges to a local minimum with short Fe-O distances. <sup>#</sup>: fixed value to prevent divergence of  $\sigma_{O1}$  to negative values.

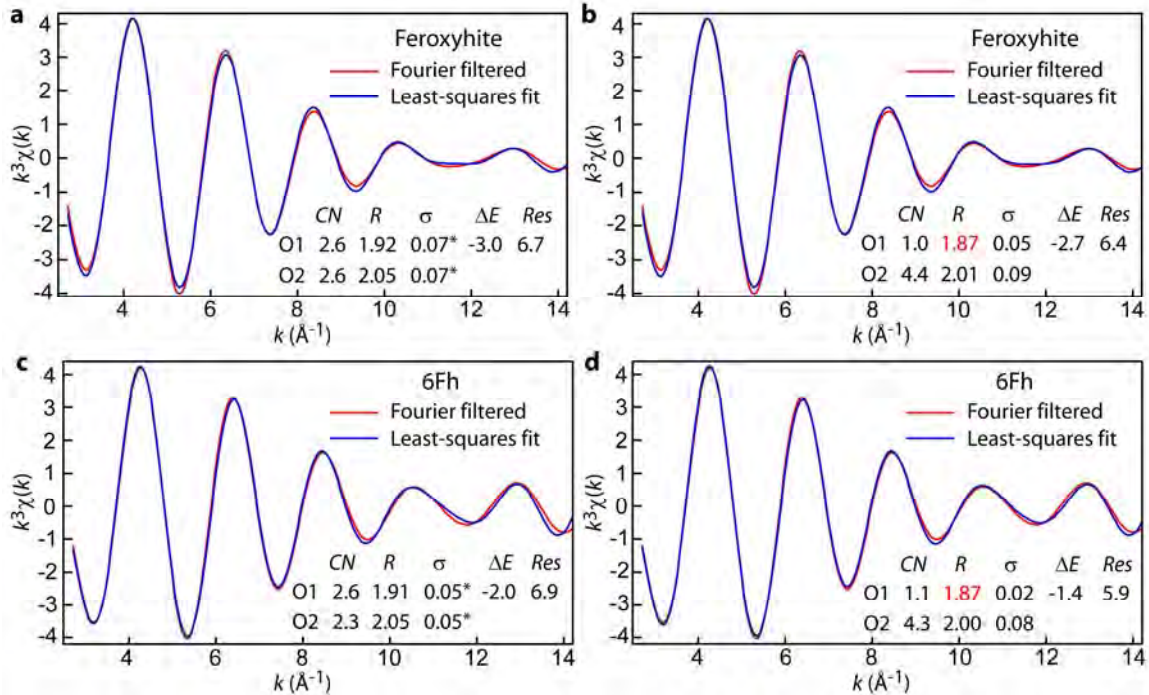


**Figure S4.** Single-shell fits of the Fourier filtered  $\chi_{\text{Fe-O}}$  function for feroxyhite and 6Fh. When  $\sigma_{O1}$  and  $\sigma_{O2}$  are optimized independently (b,d), the fit converges to  $R_{O1} = 1.87 \text{ \AA}$  and  $CN_{O1}$  exhibits a F-test value of 0.9 and the error exceeds its best-fit value (precision > 100%).

## References

- Ankudinov, A.L. and Rehr, J.J. (1997) Relativistic calculations of spin-dependent X-ray-absorption spectra. *Physical Review*, B56, 1712-1716
- Brown, I.D. and Altermatt, D. (1985) Bond-valence parameters obtained from a systematic analysis of the Inorganic Crystal Structure Database. *Acta Crystallographica*, B41, 244-247.
- De Boer, C.B. and Dekkers, M.J. (2001) Unusual thermomagnetic behaviour of haematites: neoformation of a highly magnetic spinel phase on heating in air. *Geophysical Journal International*, 144, 481-494.
- Drits, V.A., Sakharov, B.A., Salyn, A.L., and Manceau, A. (1993) Structural model for ferrihydrite. *Clay Minerals*, 28, 185-208.
- Farrow, C.L., Juhas, P., Liu, J.W., Bryndin, D., Bozin, E.S., Bloch, J., Proffen, T., and Billinge S.J.L. (2007) PDFfit2 and PDFgui: computer programs for studying nanostructure in crystals. *Journal of Physics: Condensed Matter*, 19, 335219.
- Janney, D.E., Cowley, J.M., and Buseck, P.R. (2000) Transmission electron microscopy of synthetic 2- and 6-line ferrihydrite. *Clays and Clay Minerals*, 48, 111-119.
- Janney, D.E., Cowley, J.M., and Buseck P.R. (2001) Structure of synthetic 6-line ferrihydrite by electron nanodiffraction. *American Mineralogist*, 86, 327-335.
- Liu, Q., Barron, V., Torrent, J., Eeckhout, S.G., Deng, C. (2008) Magnetism of intermediate hydromaghemite in the transformation of 2-line ferrihydrite into hematite and its paleoenvironmental implications. *Journal of Geophysical Research*, 113, 1-12.
- Manceau, A (2009) Evaluation of the structural model for ferrihydrite derived from real-space modeling of high-energy X-ray diffraction data. *Clay Minerals*, 44, 19-34.
- Manceau, A. (2010) PDF analysis of ferrihydrite and the violation of Pauling's Principia. *Clay Minerals*, 45, 225-228.
- Michel, F.M., Barrón, V., Torrent, J., Morales, M.P., Serna, C.J., Boily, J.F., Liu, Q., Ambrosini, A., Cismasu, A.C., and Brown Jr. G.E. (2010) Ordered ferrimagnetic form of ferrihydrite reveals links among structure, composition, and magnetism. *Proceedings of the National Academy of Science of the United States of America*, 107, 2787-2792.
- Pan, Y., Brown, A., Brydson, R., Warley, A., Li, A., and Powell, J. (2006) Electron beam damage studies of synthetic 6-line ferrihydrite and ferritin molecule cores within a human liver biopsy. *Micron*, 37, 403-411.
- Ressler, T. (1998) WinXAS: a program for X-ray absorption spectroscopy data analysis under MS-Windows. *Journal of Synchrotron Radiation*, 5, 118-122.
- Ressler, T., Walter, A., Scholz, J., Tessonnier, J.P., and Su, D.S. (2010) Structure and properties of a Mo oxide catalyst supported on hollow carbon nanofibers in selective propene oxidation. *Journal of Catalysis*, 271, 305-314.
- Wells, D.M., Jin, G.B., Skanthakumar, S., Haire, R.G., Soderholm, L., Ibers, J.A. (2009) Quaternary neptunium compounds: Syntheses and characterization of KCuNpS<sub>3</sub>, RbCuNpS<sub>3</sub>, CsCuNpS<sub>3</sub>, KAgNpS<sub>3</sub>, and CsAgNpS<sub>3</sub>. *Inorganic Chemistry*, 48, 11513-11517.
- Zhu W., Hausner D.B., Harrington R., Lee P.L., Strongin D.R., Parise J.B. (2011) Structural water in ferrihydrite and constraints this provides on possible structure models. *American Mineralogist*, DOI: 10.2138/am.2011.3460

**Table S1.** Confidence limits of the fitting parameters calculated from a variation of the residual (*Res*) within 90% of its optimal value

		Fe-O1			Fe-O2			Fe-Fe1			Fe-Fe2/Fe3		
		$\Delta CN$	$\Delta R$ (Å)	$\Delta \sigma$ (Å)	$\Delta CN$	$\Delta R$ (Å)	$\Delta \sigma$ (Å)	$\Delta CN$	$\Delta R$ (Å)	$\Delta \sigma$ (Å)	$\Delta CN$	$\Delta R$ (Å)	$\Delta \sigma$ (Å)
Feroxyhite – 3 <sup>rd</sup> model-fit		-	0.01	-	0.1	0.01	0.03	0.7(0.62)	0.01	-	1.0(0.80)	0.01	-
											0.8(0.70)	0.02	0.01
6Fh	- 1 <sup>st</sup> strategy	-	0.01	0.03(0.46)	0.1	0.01	0.04(0.50)	1.0(0.70)	0.02	-	1.3(0.79)	0.01	0.02
	- 2 <sup>nd</sup> strategy	-	0.01	0.03(0.48)	0.1	0.01	0.04(0.43)	1.3(0.73)	0.02	0.07(0.53)	1.1(0.72)	0.01	0.05(0.61)
6-Fh 30K – 2 <sup>nd</sup> model-fit		0.3	0.01	-	0.3(0.55)	0.05(0.68)	0.02	1.0(0.74)	0.01	0.05(0.58)	0.5(0.66)	0.008	0.04(0.63)
High-Cl akaganeite 77K		-	0.014	0.04(0.76)	0.2	0.023	0.06(0.54)	0.5(0.48)	0.01	-	0.6(0.57)	0.04	-
											0.9(0.67)	0.02	0.02

In parenthesis are correlations from the F-test. Parameters with  $0.5 < F < 0.8$  are moderately correlated and those with  $0.8 < F < 1.0$  are highly. Correlated values have higher standard deviations.